

# 1 Neural correlates of masked and unmasked tones: 2 psychoacoustics and late auditory evoked potentials 3 (LAEPs)

4 Hyojin Kim<sup>1\*</sup>, Bastian Epp<sup>1</sup>

5 <sup>1</sup>Hearing Systems Section, Department of Health Technology, Technical University of Denmark,  
6 Kgs. Lyngby, Denmark

7 \*hykim@dtu.dk

8

## 9 **ABSTRACT**

10 Hearing thresholds are commonly used to quantify a listener's ability to detect sound. In the presence of  
11 masking sounds, hearing thresholds can vary depending on the signal properties of the target and the  
12 masker, commonly referred to as auditory cues. Target detection can be facilitated with comodulated masking  
13 noise and interaural phase disparity (IPD). This can be quantified with a decrease in detection thresholds or  
14 masking release: comodulation masking release (CMR, for comodulation) and binaural masking level  
15 difference (BMLD, for IPD). As these measures only reflect the low limit of levels for target detection, the  
16 relevance of masking release at supra-threshold levels is still unclear. Here, we used psychoacoustic and  
17 electrophysiological measures to investigate the effect of masking release for a masked tone at  
18 supra-threshold levels. Behaviorally, we investigated how the amount of masking release affects the salience  
19 at supra-threshold levels. We used intensity just-noticeable difference (JND) to quantify level-dependent  
20 changes in the salience of the tonal signal. As a physiological correlate, we investigated late auditory evoked  
21 potentials (LAEPs) with electroencephalography (EEG). The results showed that the intensity JNDs were  
22 equal at the same physical target tone level, regardless of the presence or absence of masking release.  
23 Estimated salience was correlated with the amount of masking release. However, salience measures across  
24 conditions converged with the target tone level above 70 dB SPL. For the LAEPs, the P2 amplitudes were  
25 more closely linked to behavioral measures than the N1 amplitudes. Both behavioral and electrophysiological  
26 measures suggest that the salience of a masked tone at supra-threshold levels is correlated with the amount  
27 of masking release.

## 28 1. Introduction

29 Acoustic scenes in everyday life consist of a complex mixture of sounds. Our auditory system can segregate  
30 this mixture into a target sound and a noise background, enabling communication in acoustically complex  
31 environments. It is assumed that our auditory system binds various acoustic features arising from the same  
32 source into a sound object or an acoustic stream. As an example of such features, speech shows coherent  
33 amplitude modulation patterns across a wide frequency range (Raphael et al., 2007). Previous studies have  
34 shown that coherent modulation, or comodulation, is beneficial for the detection of a tone in noise (Hall et al.,  
35 1984; Nelken et al., 1999). This suggests that comodulation can be used to group spectral components across  
36 a wide range of frequency bands as comodulation indicates that these components likely stem from the same  
37 source. Such grouping can facilitate the segregation of the target signal from the noise and result in an  
38 enhanced target detection. Similarly, spatial information can also facilitate sound detection. When an acoustic  
39 source is lateralized relative to the listeners' head direction, interaural disparities between the ears can be  
40 induced. For instance, an interaural phase difference (IPD) can facilitate the target identification by grouping  
41 acoustic features from the same source. For instance, when the target tone in the noise is presented with an  
42 IPD between left and right ears, detection thresholds of the tone are lower compared to the case with no IPD  
43 (van de Par and Kohlrausch, 1999).

44 In psychoacoustics, such enhancement in detection performance is considered as "release from masking,"  
45 and referred to as masking release. Masking release can be quantified as the amount of decrease in the  
46 detection threshold in the presence of beneficial cues compared to the detection threshold obtained in the  
47 absence of these cues. A decrease in detection threshold by comodulation is termed as comodulation masking  
48 release (CMR), and the decrease related to a binaural cue is referred to as binaural masking level difference  
49 (BMLD). In simple cases where the target tone is presented with both comodulation and IPD cue, the amount  
50 of masking release was found to be a superposition of CMR and BMLD (e.g., Epp and Verhey, 2009). In  
51 their study, they interpreted the psychoacoustical measures of CMR and BMLD as the result of enhanced  
52 neural representations by bottom-up, serial neural processing. A reduced CMR in the presence of BMLD  
53 was found by Hall III et al. (2011), indicating a small interaction between the processes underlying CMR and  
54 BMLD. For CMR, the earliest physiological neural correlate of CMR was found at the CN level (Pressnitzer  
55 et al., 2001; Neuert et al., 2004). The neuronal representation of the comodulated signal gets sharper at the  
56 inferior colliculus (IC) level (Nelken et al., 1999). For BMLD, neural correlates of IPD were found at the IC level  
57 (Shackleton et al., 2003, 2005; Zohar et al., 2011). Based on these findings, Epp and Verhey (2009) suggested  
58 that the superposition of CMR and BMLD is the combination of the enhanced internal signal-to-noise ratio of  
59 the neural representations.

60 When a comodulated masker is preceded and followed by another masker (temporal fringe), CMR can be  
61 reduced or increased depending on the preceding and following maskers (Grose et al., 2009; Dau et al.,  
62 2009, 2005). It is not yet clear whether this superposition of CMR and BMLD also applies in cases where the  
63 amount of CMR is affected by the temporal context of the spectral masker components. When the temporal  
64 fringe is comodulated, CMR can be enhanced compared to the absence of the fringe (Grose et al., 2009).  
65 One interpretation of this result is that the fringe facilitates the grouping of the masker, thereby enhancing the  
66 separation of the target sound from noise. On the other hand, when the temporal fringe is uncorrelated, CMR  
67 can be reduced compared to a condition without temporal fringe (Grose et al., 2009). In this case, the fringe  
68 has a detrimental effect on the grouping of the masker, resulting in reduced CMR. Hence, these results can be  
69 linked to stream formation by frequency grouping in time, suggesting the influence of the high-level auditory  
70 processing on CMR (Grose et al., 2009; Dau et al., 2005, 2009). Neural correlates of the effect of preceding  
71 maskers on target detection were found at the cortical level (A1) (Sollini and Chadderton, 2016). In their study,  
72 neural responses to the stimuli were enhanced by a preceding comodulated masker compared to the ones  
73 preceded by an uncorrelated masker. Nevertheless, it remains unclear whether the improved neural response  
74 to the target tone at the A1 level is the result of relayed encoding from the CN to A1, or an additional encoding  
75 at the A1 level, or a cortical feedback from A1 to CN (Sollini and Chadderton, 2016). Furthermore, little is  
76 known about the effect of stream formation on the masking release induced by interaural disparities like BMLD.

77 CMR and BMLD are well characterized at low intensities (near thresholds). However, one might argue that  
78 target detection in communication occurs at levels well above threshold, i.e., supra-threshold levels. This leads  
79 to a question of the relevance of CMR and BMLD to communication in complex acoustic environments. Several  
80 studies have investigated the perception at supra-threshold levels in masking release conditions. A common  
81 goal was to map physical properties (e.g., the increment in the intensity of a sound) to psychophysical variables  
82 (e.g., the increment in loudness or salience). Related studies used categorical loudness scaling (Verhey and  
83 Heeren, 2015) and continuous scaling of the perceived salience (Egger et al., 2019). In categorical loudness

84 scaling, Verhey and Heeren (2015) used a matching method where listeners matched the loudness between  
85 the target tone in modulated noise and in unmodulated noise. The level of unmodulated noise was reduced by  
86 the amount of threshold difference between the two noise types. Their results showed that the supra-threshold  
87 perception of the target tone in the modulated noise was similar to that in the unmodulated noise at a reduced  
88 level, suggesting that the masking release results from reduced internal masker level. With continuous scaling  
89 tested on both CMR and BMLD, the data from Egger et al. (2019) showed individual variability in the ratings,  
90 presumably because some listeners confused the loudness of the overall sound with the salience of the target  
91 tone in noise. The limitation of those methods is that those measures strongly depend on listeners' subjective  
92 criteria for decision-making. As an alternative to asking listeners to quantify the salience, we used a just-  
93 noticeable difference (JND). With this method, the intensity of a target signal is decreased step-wise until the  
94 listener cannot detect the change in intensity relative to the reference signal with a fixed level (intensity JND).  
95 This approach might potentially reduce the impact of subjective criteria for judging the salience of the target  
96 tone. A previous study showed that the intensity JND follows the power law (Ozimek and Zwislocki, 1996).  
97 However, whether this relationship holds for the salience in masking release conditions is unclear.

98 As a neural correlate of an enhanced internal representation of the target tone in noise, Epp et al. (2013)  
99 evaluated auditory evoked potentials (AEPs). They hypothesized that the neural representation of the  
100 target tone in masker at the cortical level is correlated with the level above masked threshold. They assumed  
101 that the physical signal-to-noise ratio of the masked tone is enhanced by comodulation and IPD cues along  
102 the auditory pathway. The resulting enhanced neural representation of masked tone would be reflected in the  
103 peaks of the AEPs. They measured AEPs at various intensities of the tonal component with a fixed masker  
104 level. They found that the amplitude of the P2 component of the late auditory evoked potentials (LAEPs) was  
105 proportional to the amount of masking release, CMR, and BMLD. The growth function of the P2 amplitude was  
106 similar across conditions. Based on this finding, the follow-up study by Egger et al. (2019) hypothesized that  
107 LAEPs measured at the same level above masked threshold (e.g., threshold + 5 dB, + 10 dB, etc.) will evoke  
108 the same amplitude of the P2 components regardless of masking release conditions. They measured LAEPs  
109 at the six different supra-threshold levels, together with the salience of the tonal component in maskers with  
110 the scaling method. The results of LAEPs showed that the tone at the same supra-threshold levels evoked  
111 similar P2 amplitudes. However, ratings of the salience were not correlated with P2.

112 To shed light on the mechanism and neural representation of CMR and BMLD, we investigated: i) the effect of  
113 stream formation induced by preceding maskers on CMR and BMLD. We hypothesized that if stream formation  
114 results from high-level auditory processing (e.g., integration of temporal context across frequencies), both CMR  
115 and BMLD will be affected by stream formation. Understanding the interaction of bottom-up processing and  
116 the stream formation will help to reveal the neural encoding strategies underlying sound source separation.  
117 ii) the intensity JND as a measure of the "internal representation" of the tonal component in masking release  
118 conditions at supra-threshold levels. As an extension of Ozimek and Zwislocki (1996) and Egger et al. (2019),  
119 we hypothesized that the intensity JND in masking release would follow a power law as a function of supra-  
120 threshold levels, regardless of masking release conditions. If the internal neural representation is enhanced  
121 proportional to the amount of masking release, the condition with a higher amount of CMR and BMLD will  
122 show lower intensity JNDs at the same physical target tone level. iii) the correlation between the intensity  
123 JND and LAEP measures. In the present study, we estimated the slope of changes in P2 amplitudes with  
124 increased levels. We hypothesized that the increment in P2 with increasing tone level would be inversely  
125 proportional to the intensity JND. In addition, based on the intensity JND measures, we estimated the salience  
126 and investigated whether P2 can reflect the estimated salience behaviorally.

## 127 **2. Materials and methods**

### 128 **2.1. Stimuli**

129 Our study consisted of three experiments: i) psychoacoustical threshold measurements to quantify CMR and  
130 BMLD; ii) intensity JND measurements; iii) EEG experiments for measuring LAEPs. For all three experiments,  
131 we used the same eight masking release conditions (Fig 1). The stimulus consisted of five noise bands as a  
132 masker and a pure tone as a target signal: one noise band was centered at the frequency of the target tone  
133 (center band, CB). The other bands were equally spaced with a distance of 120 Hz above and below the CB  
134 (flanking bands, FBs). Each masker band had a bandwidth of 20 Hz and a level of 60 dB SPL. The target  
135 tone was centered at 700 Hz. We chose this frequency setting to maximize the effect of the stream formation  
136 on CMR based on the previous work by Grose et al. (2009). Each interval consisted of a preceding masker  
137 with a duration of 500ms ("preceding masker") and a masked target tone with a duration of 200ms ("masked  
138 tone interval"). We used four masker conditions. In the reference condition, the maskers had random intensity

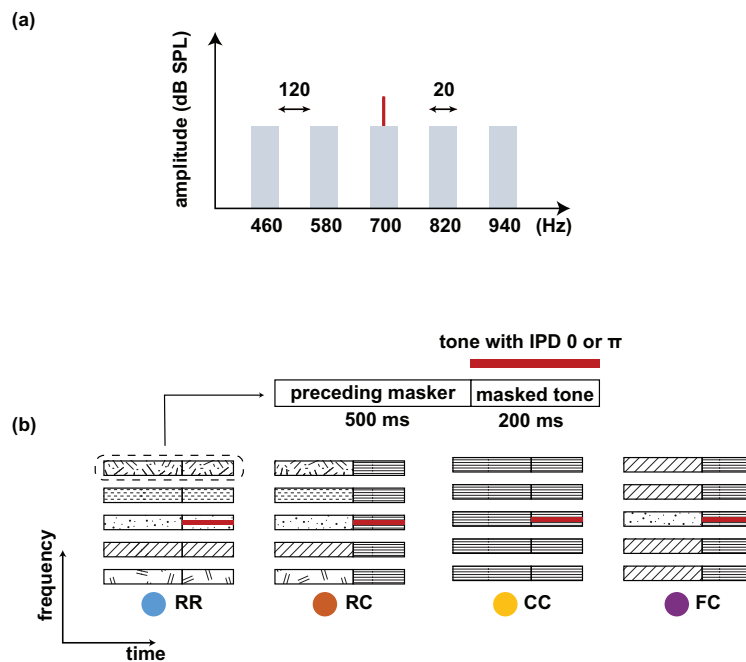


**Fig 1: (a) Spectra of the stimulus. A target tone (700 Hz) was presented with a masking noise consisting of five narrow-band maskers: One band centered at the target tone frequency (center band, CB) and four flanking bands (FBs). The bandwidth of each masker band was 20 Hz, and the frequency spacing between FBs was 120 Hz. The overall level of the noise was set to 60 dB SPL. (b) Schematic spectrograms of the stimuli. Each stimulus consists of a preceding masker (500 ms) and masked tone (200 ms). Four types of maskers were used: RR, RC, CC, and FC. The RR was used as the reference condition with uncorrelated masker bands. In the other three conditions, the maskers consisted of a comodulated masker preceded by three different maskers: uncorrelated masker (RC), comodulated masker (CC), and the masker with comodulated flanking-bands (FC). The thick red line represents a tone that was presented with an IPD of 0 or  $\pi$ .**

139 fluctuations across frequency for both the “preceding masker” and the “masked tone interval” (RR). In the three  
 140 other conditions, the target tone was embedded in comodulated noise and preceded by one of the following  
 141 masker types: a masker with random intensity fluctuations across frequency (RC), a comodulated masker  
 142 (CC), and a masker where only the FBs were comodulated (FC). All maskers were presented diotically and  
 143 had 20 ms raised-cosine on- and offset ramps. For RC and FC conditions, the same on- and offset ramps  
 144 were added in the transition with a 50% overlap. The noise bands were generated in the frequency domain  
 145 and transformed into the time domain. The noise bands were assigned numbers from a uniformly distributed  
 146 random process to the real and imaginary parts of the respective frequency components. For the R masker,  
 147 different numbers were assigned for each noise band. For the C masker, the same numbers were used for all  
 148 five noise bands. The stimuli were generated with newly drawn numbers for each interval and each trial. To  
 149 induce BMLD, the target tone was presented with an IPD of 0 or  $\pi$  in combination with the same four masker  
 150 types, leading to a total of eight stimulus conditions.

## 151 2.2. Apparatus

152 During all three experiments, the listeners were seated in a double-walled, soundproof booth. All stimuli were  
 153 generated in MATLAB 2018b (TheMathworks, Natick, MA) with a sampling rate of 44100 Hz and a 16-bit  
 154 resolution, converted from digital to analog (RME Frieface UCX), amplified (Phonitor mini, SPL electronics),  
 155 and played back through headphones (ER-2, Etymotic Research). The headphones were calibrated at the  
 156 signal frequency of the tone. For the recording of AEPs, we used a g.Tec Hlamp system with a sampling rate  
 157 of 1024 Hz. The 64 channels of active electrodes were set up with highly conductive electrode gel to reduce

158 the impedance between the scalp and electrodes. The reference electrodes were placed close to the mastoid  
159 of both ears and the other electrodes were placed based on g.GAMMAcap 64 channel setup from g.Tec.

## 160 **2.3. Listeners**

161 We recruited fifteen normal-hearing listeners. None of them reported any history of hearing impairment. All  
162 but one listener had pure-tone hearing thresholds within 15 dB HL for the standard audiometric frequencies  
163 from 125 to 4000 Hz. One listener was tested with 20 dB at 125 Hz. All participants provided informed  
164 consent, and all experiments were approved by the Science-Ethics Committee for the Capital Region of  
165 Denmark (reference H-16036391). All of them participated in the first experiment, eleven of them participated  
166 in the second experiment, and ten of them participated in the third experiment.

## 167 **2.4. Procedure**

168 In the first experiment, we measured masked thresholds individually for the eight stimulus conditions presented  
169 in random order. We used an adaptive, three-interval, three-alternative forced-choice procedure (3-AFC) with  
170 a one-up, two-down rule to estimate the 70.7% of the psychometric function (Ewert, 2013; Levitt, 1971). Two  
171 intervals contained the masking noise only. The remaining interval contained the target tone in addition to  
172 the masker. The three intervals were presented with a temporal gap of 500 ms in between. The listeners'  
173 task was to select the interval with the target tone by pressing the corresponding number key (1, 2, 3) on the  
174 keyboard. Visual feedback was provided, indicating whether the answer was "WRONG" or "CORRECT". The  
175 initial level of the target tone was set to 75 dB SPL and was adjusted with an initial step size of 8 dB. The step  
176 size was halved after each lower reversal until it reached the minimum step size of 1 dB. The signal level at a  
177 minimum step size of 1 dB was measured six times, and the mean of the last six reversals was used as the  
178 estimated threshold. Each listener performed three threshold measurements for all conditions. The average  
179 of three measurements was used as individual masked thresholds for the next two experiments. Additional  
180 measurements were performed if the thresholds from the last three measurements had a standard deviation  
181 larger than 3 dB.

182 In the second experiment, we measured intensity JNDs individually at six supra-threshold levels for all  
183 conditions. The intensity of the tone was individually adjusted for each listener to match levels of +0 dB  
184 (threshold), +5 dB, +10 dB, +15 dB, +20 dB, and +25 dB relative to the threshold. The individual mean of  
185 three threshold measurements from the first experiment was used to set the reference of +0 dB. We used the  
186 same setup and 3-AFC method as for the first experiment. Two intervals contained the masked target tone  
187 with a fixed level at one of the supra-threshold levels ("reference interval"), and the remaining interval  
188 contained the masked target tone with a higher level than the others ("target interval"). The intervals were  
189 presented with a temporal gap of 500 ms in between. Listeners were asked to select the interval with the tone  
190 of highest intensity by pressing the corresponding number key (1, 2, 3) on the keyboard. Visual feedback was  
191 provided, indicating whether the answer was "WRONG" or "CORRECT." The order of conditions and  
192 supra-threshold levels were randomized. The initial level of the tone in the target interval was set to  
193 75 dB SPL. The level of the target tone was adjusted with the initial step size of 8 dB. The step size was  
194 halved after each lower reversal until it reached the minimum step size of 1 dB. The signal level at a minimum  
195 step size of 1 dB was measured six times, and the mean of the last six reversals was used as the JND.  
196 Listeners were familiarized with the task by a test run. Each listener performed three trials for all conditions. If  
197 the supra-threshold level exceeded 80 dB, the intensity JND measure was skipped. We calculated the  
198 intensity JND by subtracting the level of "reference intervals" from the minimum level of discriminable tone in  
199 "the target interval".

200 In the third experiment, we measured late auditory evoked potentials (LAEPs) at three supra-threshold levels  
201 for all conditions. The intensity of the tone was individually adjusted for each listener to match levels of +15  
202 dB, +20 dB, and +25 dB above the threshold. The individual mean of three threshold measurements from the  
203 first experiment was used to set supra-threshold levels. The stimuli for each condition and supra-threshold  
204 level were presented 400 times in random order. In addition, noise-only stimuli were presented 40 times for  
205 each condition. The presentations were separated by a random inter-stimulus interval of 500ms with jitter.  
206 During the experiment, a silent movie with subtitles was presented on a low-radiation screen. The listeners  
207 were asked to sit comfortably and avoid movement as much as possible. The experiment was divided into six  
208 blocks of approximately 38 minutes each. These were divided into two sessions on different days.

## 209 Data analysis

210 **The threshold measurements** We used CMR and BMLD to quantify the amount of masking release in eight  
211 conditions. We used several acronyms for masking release measures for each condition as follows. For  
212 comodulation masking release (CMR),

$$\text{CMR}_{m/ipd} = \text{threshold}[\text{RR}_{ipd}] - \text{threshold}[m_{ipd}], \quad (1)$$

213 Here,  $m$  stands for one of three masker types (RC, CC, FC) and  $ipd$  stands for the IPD of the tone between two  
214 ears (0 or  $\pi$ ). As an example,  $\text{CMR}_{CC\pi}$  is the amount of a decrease in threshold in  $CC\pi$  condition compared  
215 to  $\text{RR}\pi$  condition. A positive value indicates a decreased detection threshold, and a negative value indicates a  
216 increased detection threshold. For binaural masking level difference (BMLD),

$$\text{BMLD}_m = \text{threshold}[m_0] - \text{threshold}[m_\pi], \quad (2)$$

217 Here,  $m$  stands for one of three masker types (RC, CC, FC). As an example,  $\text{BMLD}_{CC}$  is the amount of a  
218 decrease in threshold in  $CC$  condition with IPD of  $\pi$  compared to  $CC$  condition without IPD. For statistical  
219 analysis, the Lilliefors test was used for a normality test. To compare CMR and BMLD across four masker  
220 types, one-way ANOVA followed by Tukey's multiple comparison tests were used. In the case where the data  
221 did not follow a normal distribution, the Kruskal–Wallis test was used, followed by Dunn's multiple comparison  
222 test. To compare CMR between two conditions with the same masker type but with different IPD, Wilcoxon  
223 signed-rank test was used.

224  
225 **Intensity JNDs** We calculated the intensity JND by subtracting the intensity level of the reference intervals  
226 from the minimum intensity level of the discriminable tone in the target interval ( $\Delta L$ ). We fitted JND measures  
227 for each condition with a power law. In addition, we estimated the Weber fraction  $k$  by dividing the intensity  
228 JND ( $\Delta L$ ) with the intensity level of the target tone ( $L$ ). We also calculated  $10\log(\Delta L/L)$ . From the fitted  
229 intensity JNDs, we estimated the salience from 1 to 10 (arbitrary scale). For each condition, we assumed that  
230 the salience was one at the corresponding masked thresholds. We increased the salience by one when the  
231 level was increased by the intensity JND at the current level. We repeated this estimation until the salience  
232 reached ten.

233  
234 **Late auditory evoked potentials (LAEPs)** Collected data were analyzed using FieldTrip (Oostenveld et al.,  
235 2011). In short, the EEG data were partitioned into epochs from -300 to 850 ms relative to the onset of the  
236 preceding masker. The region of interest was the central position (Gz), and the reference signals were the  
237 average of two electrodes near the mastoids. Each epoch was low-pass (Butterworth IIR filter, 6th order, zero-  
238 phase) filtered with a cut-off frequency of 20 Hz. Detrending, baseline correction, and weighted averaging were  
239 applied to increase the signal-to-noise ratio (Riedel et al., 2001). Trials containing signals exceeding 100  $\mu\text{V}$  in  
240 any channel were rejected as artifacts. For auditory evoked potentials (AEPs), we extracted the signals from  
241 100 ms before the onset of the target tone and 100 ms after the offset of the target tone from the averaged  
242 epochs. Baseline correction was applied considering a 100 ms pre-stimulus period. The grand mean of AEPs  
243 was computed with arithmetic mean over all individual AEPs. We selected the first negative component (N1)  
244 and the second positive component (P2) as a peak measure individually. We defined the peak of the first  
245 negative deflection in the time window between 100 ms and 200 ms (with respect to the target onset) as N1  
246 and the peak of the second positive deflection in the time window between 200 ms and 300 ms as P2. This  
247 was estimated for each individual AEPs to eliminate individual differences in latency. Peak amplitudes were  
248 extracted by the MATLAB function *findpeaks* by locating minima and maxima within the time frame defined for  
249 N1 and P2, respectively. Extracted LAEPs were visually verified. In the case where multiple components were  
250 found, the one with the largest amplitude was selected. When there was no component found, this condition  
251 was excluded from the analysis.

### 252 3. Results

#### 253 3.1. Experiment 1. Masked thresholds

254 Fig 2a shows the mean masked thresholds for eight stimulus conditions. For an IPD of 0, thresholds were  
255 highest for the FC condition and lowest for the CC condition. The observed mean threshold across all the  
256 participants for the  $RR_0$  condition was 55.4 dB. The  $RC_0$  condition had a mean threshold of 52.2 dB. In the  
257  $CC_0$  condition, the threshold was 45.7 dB. In the  $FC_0$  condition, the mean threshold was found to be 58.7 dB.  
258 The same overall pattern of the thresholds was found for an IPD of  $\pi$  with the highest threshold for the FC  
259 condition and the lowest for the CC condition. The  $RR_\pi$  had a mean threshold of 39.5 dB, and the  $RC_\pi$   
260 condition had a mean threshold of 38.3 dB. In the  $CC_\pi$ , the mean threshold was 33.1 dB, and that of the  $FC_\pi$   
261 condition was 45.7 dB.

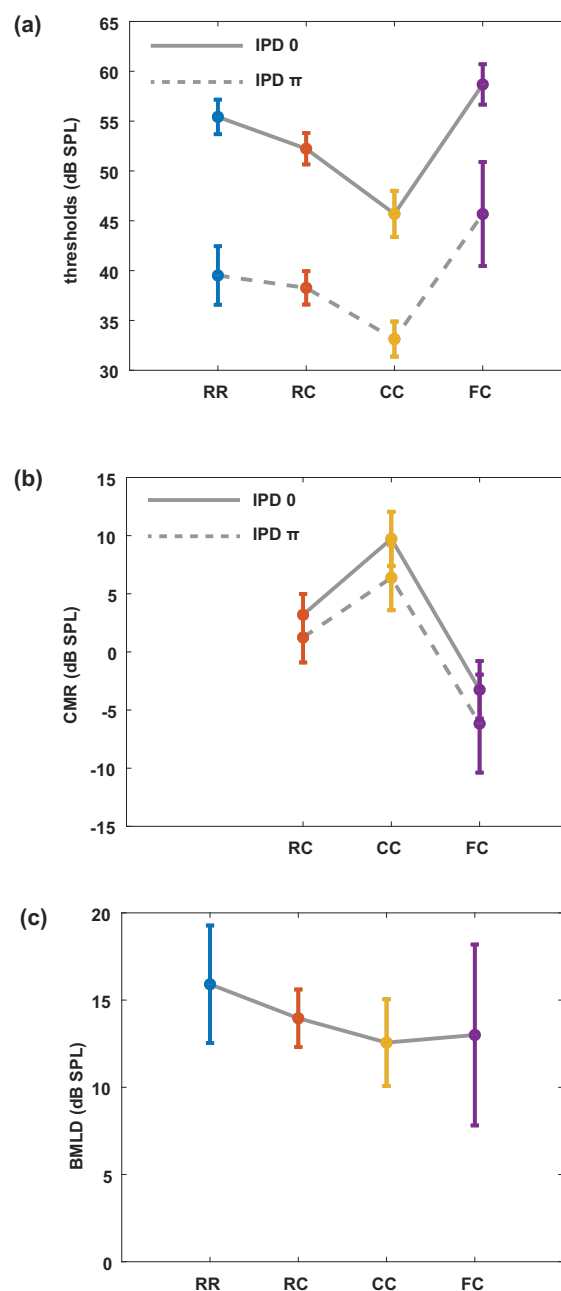


**Fig 2: Mean masked thresholds for all conditions and masking releases. (a) Masked thresholds from eight masking release conditions averaged over all listeners. (b) CMR with the RR masker as a reference. (c) BMLD for all masker types. Error bars indicate plus-minus one standard deviation.**

262 Fig 2b shows the CMR calculated for each condition by using the RR condition as reference (eq. (1)). The CMR  
263 was highest in CC conditions. While the CMR were positive for RC and CC conditions, FC conditions showed  
264 negative CMR. In the diotic conditions,  $CMR_{RC0}$  was 3.2 dB,  $CMR_{CC0}$  was 9.7 dB and  $CMR_{FC0}$  was -3.3 dB.  
265 In dichotic conditions,  $CMR_{RC\pi}$  was 1.2 dB,  $CMR_{CC\pi}$  was 6.4 dB and  $CMR_{FC\pi}$  was -6.2 dB. Statistical  
266 analysis showed that CMR measures were different between different masker types. In diotic conditions, there  
267 was a significant difference in CMR between masker types (Kruskal-Wallis,  $p < 0.05$ ). Likewise, in dichotic  
268 conditions, CMR was significantly different between masker types (Kruskal-Wallis,  $p < 0.05$ ). Between diotic  
269 and dichotic conditions with the same masker type, all masker types showed a significant difference (Wilcoxon  
270 signed-rank test,  $p < 0.05$ ). Fig 2c shows the BMLD calculated for each condition by using the threshold in  
271 the corresponding diotic condition as reference (eq. (2)).  $BMLD_{RR}$  was 15.9 dB,  $BMLD_{RC}$  was 13.9 dB,  
272  $BMLD_{CC}$  was 12.6 dB, and  $BMLD_{FC}$  was 13 dB. Multiple comparison tests showed that the  $BMLD_{RR}$  and  
273  $BMLD_{CC}$  were significantly different (one-way ANOVA,  $p < 0.05$ ).

### 274 3.2. Experiment 2. Intensity JNDs

275 Fig 3 shows the individual intensity JND measures as the function of the physical target tone level in the  
276 reference signal. Each panel shows the intensity JND measures at supra-threshold levels ranging from  
277 threshold (+ 0 dB) to + 25 dB in four masker types with both IPD of 0 (solid line) and IPD of  $\pi$  (dashed line).  
278 For each masker type, the intensity JND measures were fitted with a power function. Additionally, the intensity  
279 JND measures ( $\Delta L$ ) were re-scaled as  $10\log(\Delta L/L)$ , and fitted with a power function (Fig 4). Overall,  
280 conditions with lower detection thresholds (e.g.,  $CC_{\pi}$ ) showed higher JNDs compared to those with higher  
281 detection thresholds (e.g.,  $RR_0$ ). This indicates that the degree of enhancement in the salience depends on  
282 the target tone level rather than the supra-threshold level. Fig 5 shows the averaged intensity JND (left) and  
283 re-scaled JND (right) as the function of the physical target tone level in the reference signal. The intensity  
284 JND measures of all conditions and listeners are shown with scatter plots and fitted with the power function.  
285 The intensity JNDs decreased with an increasing level of the target tone in all masking release conditions.  
286 Re-scaled JND measures showed better goodness of fit with the power function.

287  
288 **Estimated salience** We define salience in the context of this study as the perceptual quantity that describes  
289 how clear the tone is perceived in noise. Assuming that the salience is the same as one at the threshold level,  
290 the salience would increase as the level of the target tone is increased. We hypothesized that the salience  
291 rating would increase by one the target tone level is increased by the intensity JND. The estimated salience  
292 is shown in Fig 6. At the same physical target tone level, estimated salience was higher for conditions with  
293 lower detection thresholds. For instance, the salience was higher in dichotic conditions compared to the diotic  
294 conditions with the same masker type. Estimated salience converged when the target tone level was above  
295 around 70 dB SPL.

### 296 3.3. Experiment 3. Late auditory evoked potentials

297 Fig 7a shows the grand mean AEPs across all listeners for each condition. The plot shows the AEPs to  
298 diotic signals (solid lines) and dichotic signals (dashed lines) in the four masker types  $RR$ ,  $RC$ ,  $CC$ , and  $FC$ ,  
299 respectively. Following the onset of the stimuli (Fig 7a, blue line), an onset response was elicited, which went  
300 back to a constant value after around 300 ms post-onset. The response to the target signal was found from  
301 around  $t=550$  ms. Fig 7b shows the mean of LAEPs across all listeners for each condition. A characteristic  
302 LAEP wave morphology was found for all masker types with a small positive deflection (P1), followed by a large  
303 negative deflection (N1) and a large positive deflection (P2). Fitted N1 and P2 amplitudes as a function of the  
304 target tone level are shown in Fig 8 and 9, respectively. Each panel shows the LAEPs of each masker type  
305 with both diotic (solid lines) and dichotic (dashed lines) target tones. As shown in Fig 10, both components  
306 showed an increase in amplitudes with increasing levels. Compared to N1, P2 amplitudes showed better  
307 goodness of fit for the power law function. In addition, N1 amplitudes showed more separation between diotic  
308 and dichotic conditions compared to P2 amplitudes.

## 309 4. Discussion

### 310 4.1. Effect of preceding maskers on CMR and BMLD

311 The results of the first experiment (Fig 2) showed that comodulation, IPD, and the preceding masker all  
312 influence the amount of masking release. In both diotic and dichotic conditions, the effect of preceding  
313 maskers on CMR was similar, as shown in Fig 2b. The amount of CMR (Fig 2b) was highest for the condition



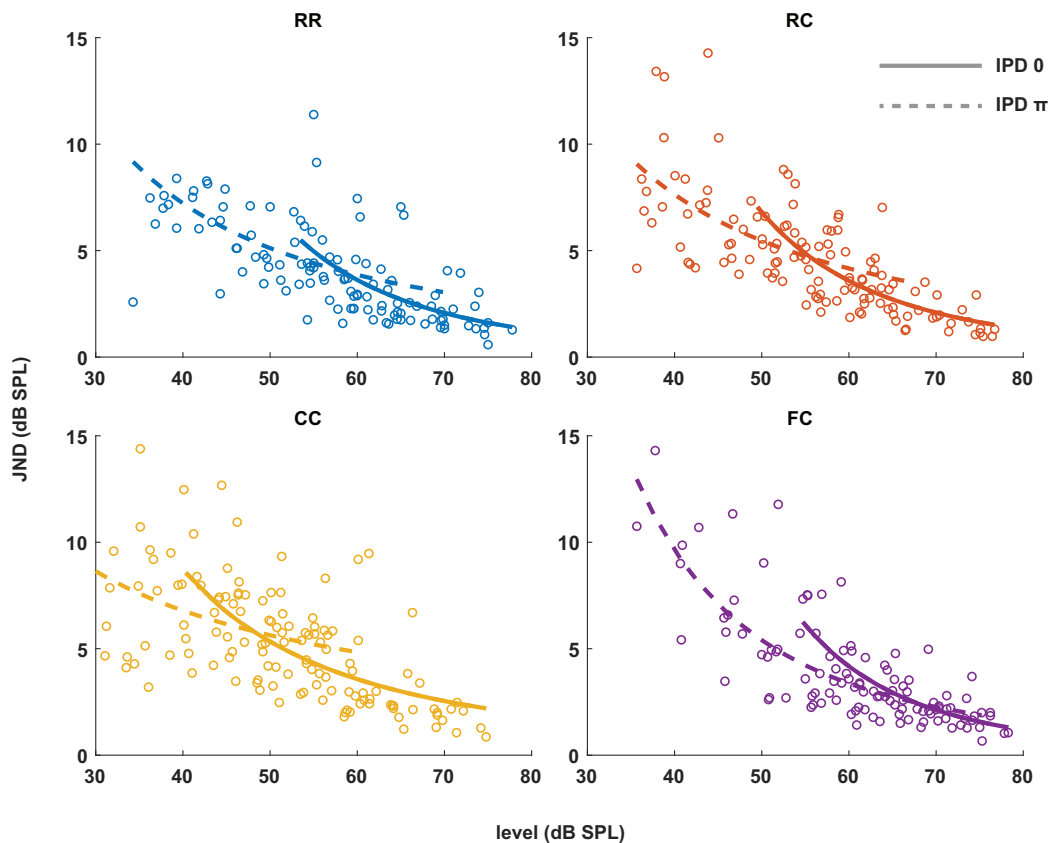


**Fig 3: Intensity JNDs for all stimulus conditions and power law fit for diotic (solid line) and dichotic target signal (dashed line). Individual data are plotted as single points. The data for each condition are fitted with a power function. Each color represents four masker types. Solid lines represent diotic conditions (IPD of 0) and dotted lines represent dichotic conditions (IPD of  $\pi$ ). The goodness of fit for each condition with IPD of 0 was: RR( $R^2=0.4748$ ), RC( $R^2=0.6614$ ), CC( $R^2=0.4732$ ), FC( $R^2=0.5604$ ). The goodness of fit for each condition with IPD of  $\pi$  was: RR( $R^2=0.2743$ ), RC( $R^2=0.1613$ ), CC( $R^2=0.2946$ ), FC( $R^2=0.6170$ ).**

314 where the masker was comodulated for the whole duration of the interval (*CC*). CMR was reduced if the  
 315 preceding masker had uncorrelated intensity fluctuations across frequency (*RC*). CMR was negative in the  
 316 condition where comodulation of the preceding masker only spanned the FBs (*FC*). In a previous study by  
 317 Grose et al. (2009), when the target tone was preceded and followed by maskers (temporal fringe), similar  
 318 results were found. They interpreted the results in the light of the formation of a stream facilitated by the  
 319 preceding masker. Even though the stimuli in the present study had no following masker after the offset of the  
 320 target tone, the thresholds were in line with the results in (Grose et al., 2009) with both preceding and  
 321 following maskers in a CMR paradigm. This suggests that the preceding masker plays a strong role in  
 322 inducing auditory streams, which may impede the following stream formation by comodulation. This is also  
 323 consistent with studies where the reduction of CMR by preceding or following stream formation was  
 324 suggested as a high-level auditory processing (Dau et al., 2005, 2009). In addition, CMR was significantly  
 325 reduced in dichotic conditions (e.g.,  $CC_0$  vs.  $CC_\pi$ ). This is also in line with previous studies by (Schooneveldt  
 326 and Moore, 1989; Cohen and Schubert, 1991; Ernst and Verhey, 2006; Epp and Verhey, 2009).

327 While the effect of preceding maskers on CMR was strong, its effect on BMLD was less pronounced. The  
 328 amount of BMLD (Fig 2c) was similar across conditions and only showed a significant difference between the  
 329 RR and the CC condition. The BMLD in the *CC* condition was lower compared to the *RR* condition. A potential  
 330 reason for this reduced BMLD could be that the overall improvement of the target signal by comodulation and  
 331 IPD reached a maximum. A similar phenomenon was observed in Epp and Verhey (2009) where listeners with  
 332 a high BMLD showed slightly reduced CMR. Interestingly, the *FC* condition showed high individual variability in

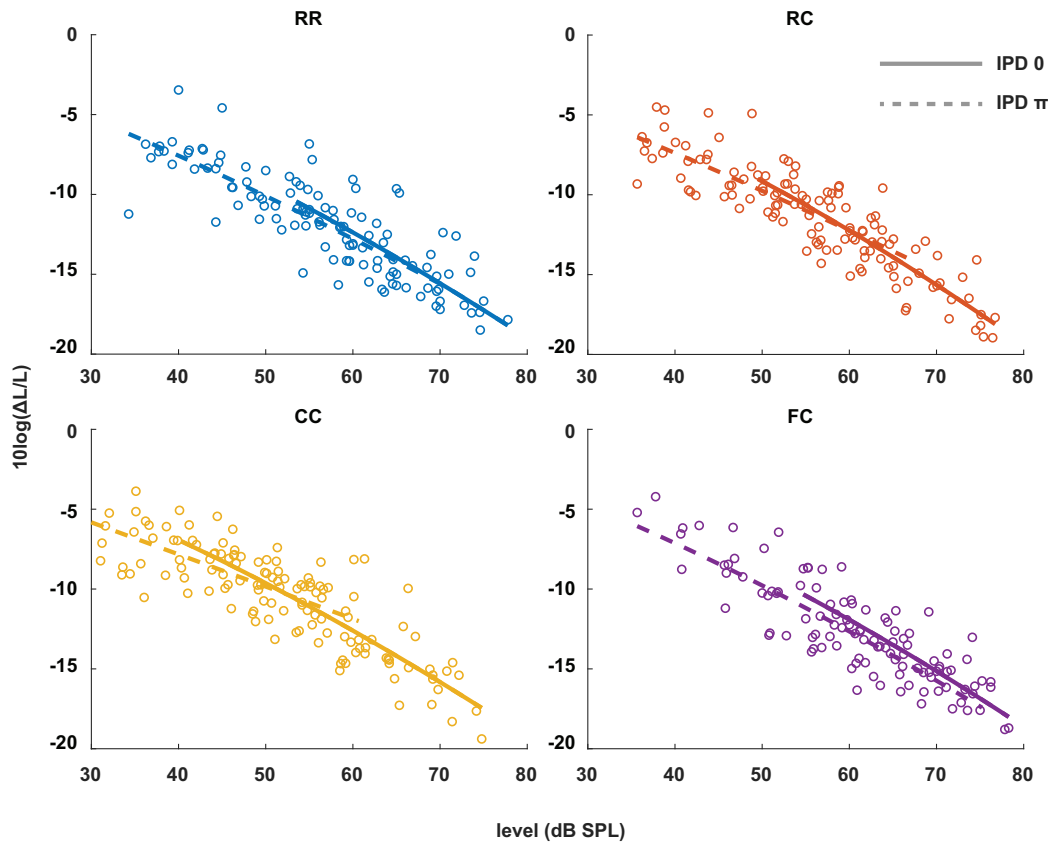


**Fig 4: Re-scaled intensity JND measures.** Individual data are plotted as single points. The data for each condition are fitted with a power function in the same manner as the Fig 3. The goodness of fit for each condition with IPD of 0 was: RR( $R^2=0.6386$ ), RC( $R^2=0.7914$ ), CC( $R^2=0.7472$ ), FC( $R^2=0.6491$ ). The goodness of fit for each condition with IPD of  $\pi$  was: RR( $R^2=0.6338$ ), RC( $R^2=0.6316$ ), CC( $R^2=0.4993$ ), FC( $R^2=0.7559$ ).

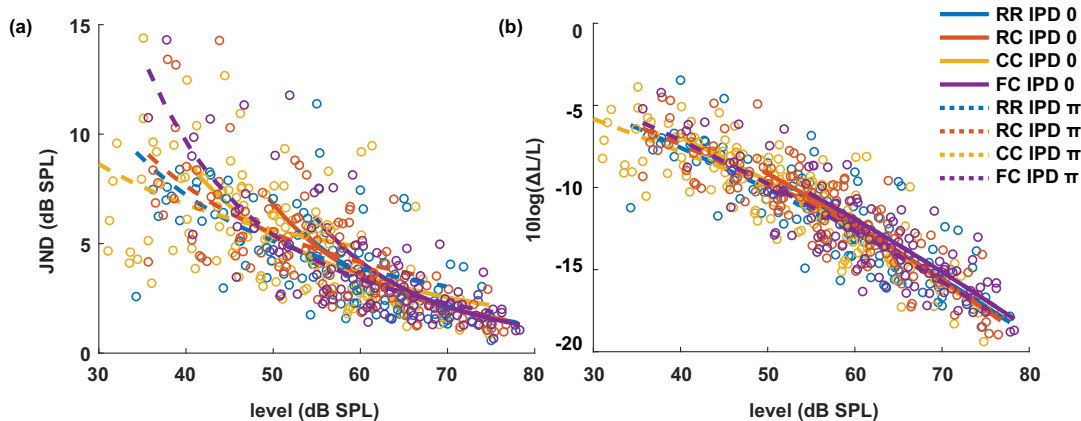


**Fig 5: (a) The intensity JND measures. (b) Re-scaled intensity JND measures across all conditions.**

333 detection thresholds when the tone was presented with an IPD of  $\pi$ . From additional linear regression analysis  
 334 (Fig 13), the *FC* condition in dichotic condition showed positive relation between CMR and BMLD. For listeners  
 335 with low CMR and BMLD, the FBs and the CB might have been separated into different objects by comodulated  
 336 FBs in the preceding masker. This may induce difficulties in separating the center masker from the tone due

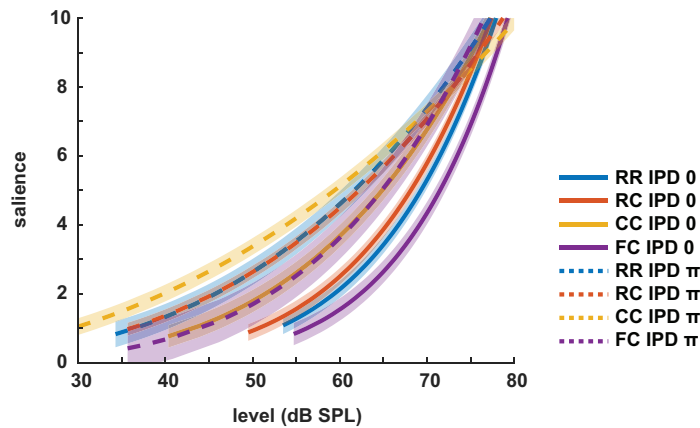


**Fig 6: Estimated saliency ratings. Each color represents four masker types. Solid lines represent diotic conditions (IPD of 0) and dotted lines represent dichotic conditions (IPD of  $\pi$ ). The shaded areas indicate  $\pm$  one root mean square error.**

337 to its tone-like perceptual quality, especially when the target tone is presented at levels as low as 45 dB. For  
338 listeners with high CMR and BMLD, if they focused on the IPD cue, spatial information effectively separated  
339 the target tone from the noise and the noise components with no interaural disparity were grouped into one  
340 stream. However, this needs to be further investigated how the individual variability occurs.

341 We hypothesized that the preceding maskers would affect both CMR and BMLD if the effect of auditory object-  
342 stream formation on masking release is due to higher-level auditory processing where prior knowledge  
343 affects sound perception. As previously mentioned, physiological evidence shows that neural correlates of  
344 comodulation processing can be found as early as the CN level (Pressnitzer et al., 2001; Neuert et al., 2004),  
345 while there is broad consensus that binaural information is processed at the level of the IC (e.g. Shackleton  
346 et al., 2003, 2005; Zohar et al., 2011). Under the assumption of bottom-up processing of the masked signal  
347 along the auditory pathway, beneficial auditory cues enhance the internal representation of the target signal  
348 at the brainstem level (CN, IC), inducing masking release. Hence, if the effect of the preceding maskers is  
349 the additional high-level auditory processing, on top of the brainstem level processing, this would affect the  
350 combined CMR and BMLD. In this study, the data suggest that BMLD is hardly affected by preceding maskers,  
351 while CMR varies strongly dependent on the type of preceding masker. This is not in agreement with the  
352 interpretation that the effect of preceding maskers is the result of high-level auditory processing (e.g., temporal  
353 integration).

354 A possible explanation is the top-down processing where prior knowledge about the sound is used to influence  
355 the processing of sensory information at the low-level (Asilador and Llano, 2021). In this scenario, the auditory  
356 system uses accumulated information of incoming sound, which can be understood as adaptation at a "system-  
357 level". This adaptation at the cortical level could affect auditory processing at the brainstem. Such an auditory  
358 efferent system from the auditory cortex to the CN could explain the effect of preceding maskers on CMR but  
359 not BMLD (Terroros and Delano, 2015). However, the neural correlates for the top-down modulation arising  
360 from the preceding maskers are unknown.

361 Lastly, one might also speculate about the role of adaptation processes at the peripheral level in the effect of  
362 preceding maskers. Similar to the paradigm used in this study, various psychophysical and neural phenomena  
363 have shown the influence of preceding signals on the following target tone perception, termed as "auditory  
364 enhancement" (e.g. Nelson and Young, 2010; Kreft et al., 2018). In these studies, the preceding maskers  
365 were broadband noise with a spectral notch around the target signal. The presence of a spectral gap around  
366 the signal frequency in the preceding masker enhanced the target detection. The underlying mechanism of  
367 "auditory enhancement" has been attributed to the adaptation at both low- and high-level auditory processing.  
368 For supporting the adaptation at low-level auditory processing, Kreft et al. (2018) suggested that olivocochlear  
369 efferents may induce the adaptation effect in a longer time scale than the auditory nerve fibers (Guinan Jr,  
370 2006). If this is the case, how modulation patterns (e.g., *RR*, *RC*, *CC*, and *FC*) result in different degrees of  
371 CMR reduction is in question. Based on a physiological study where modulation pattern encoding was found  
372 at the CN level, the connectivity between the CN and the medial olivocochlear (MOC) efferents may play a role  
373 (Pressnitzer et al., 2001; Oertel et al., 2011). However, further psychoacoustic and physiological studies are

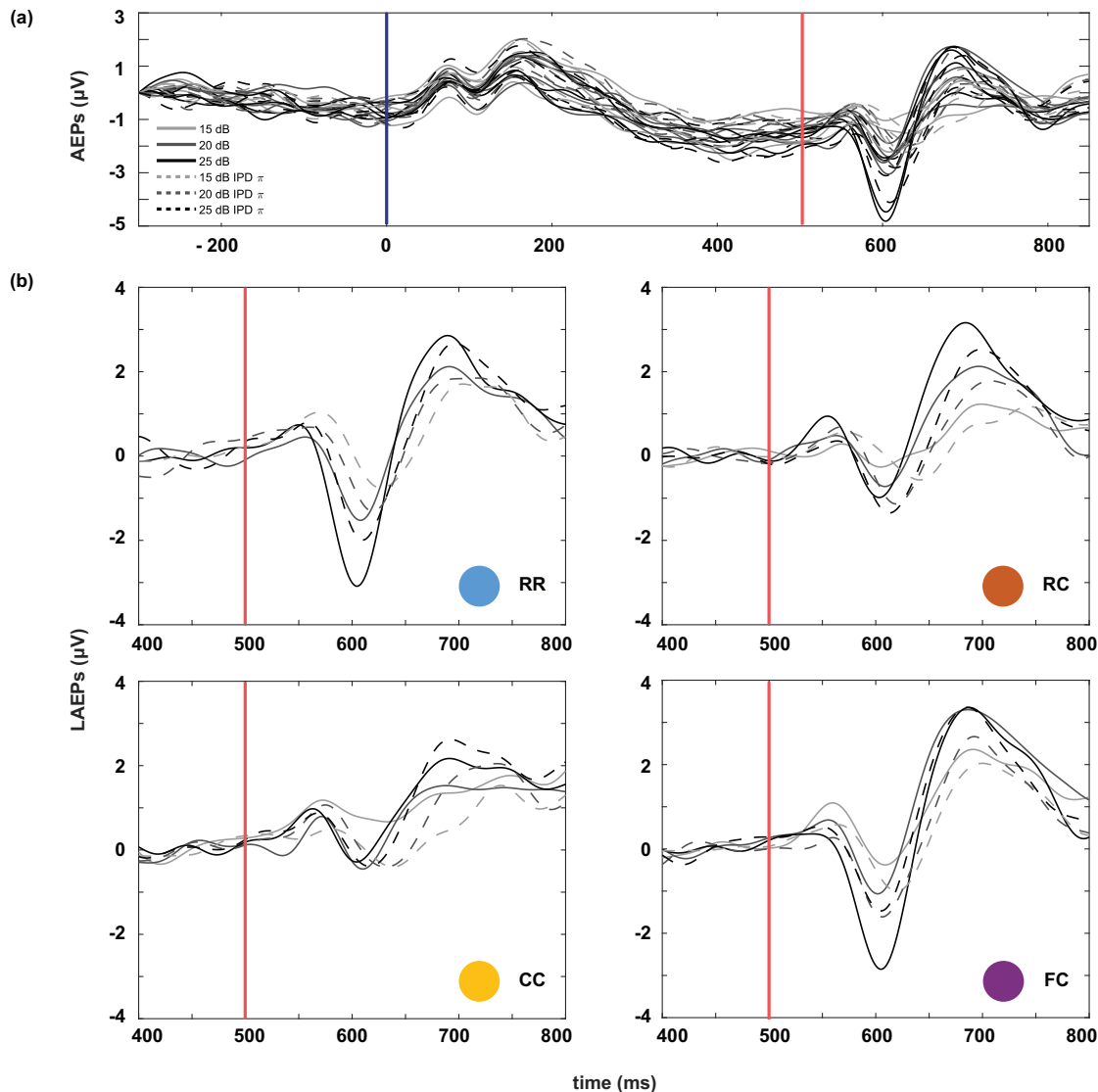


**Fig 7: Auditory evoked potentials (AEPs) averaged over all listeners. Masker onset is at  $t=0$ , target tone onset at  $t = 500$  ms. Solid lines represent the four masker types with diotic target signals, and the dotted lines represent the four masker types with dichotic target signals. (b) Late auditory evoked potentials (LAEPs) to the target tone in the time interval ranging from 400 ms to 800 ms post masker onset.**

374 needed to develop current ideas.

## 375 4.2. Benefit of CMR and BMLD at supra-threshold levels

376 The results of the second experiment (Fig 3) showed that the intensity JND was inversely proportional to  
 377 the physical sound level. This is consistent with data from the literature for pure tones in quiet (e.g. Ozimek  
 378 and Zwislocki, 1996) where the intensity JND decreased according to the power function of sensation level.  
 379 Expression of the JND on a relative scale to the reference level ( $10\log(\Delta L/L)$ ) showed independence of the  
 380 JND on the masker type ( $RR$ ,  $RC$ ,  $CC$ ,  $FC$ ) and the IPD ( $0$ ,  $\pi$ ). This means that, for a given target tone level,  
 381 regardless of the difference in masked thresholds, the intensity JND on a relative scale was the same. Such  
 382 level dependency of JND is interesting in terms of the level above the masked threshold or the supra-threshold  
 383 level. Between two conditions, the level above masked threshold can differ by up to 25 dB at a given target tone  
 384 level ( $FC_0$  vs.  $CC_\pi$ ). While the target tone level of 70 dB SPL is just above the threshold for the FC masker  
 385 and well above the threshold for the CC masker. Still, for both cases, the same relative amount of intensity

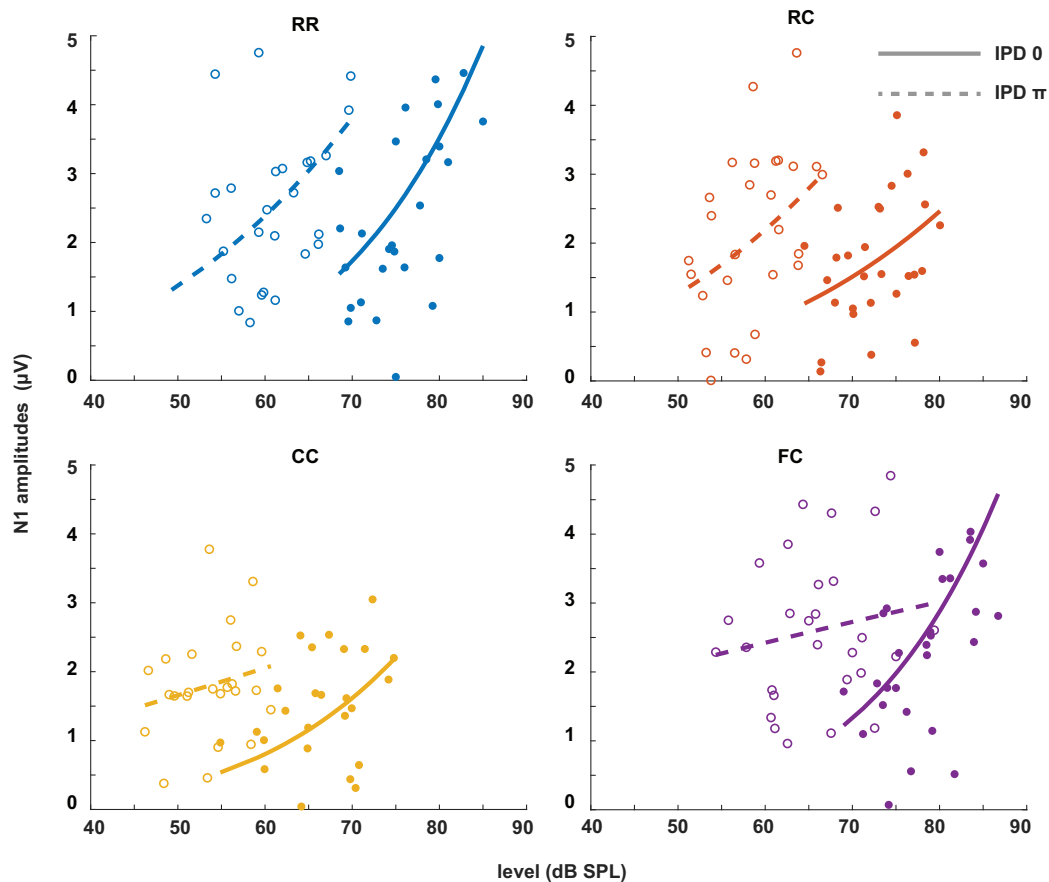


**Fig 8: N1 amplitudes as a function of target tone level at supra-threshold levels: + 15 dB, + 20 dB and + 25 dB. Individual data are plotted as single points. The data for each condition are fitted with a power function (line). Blue represents the RR condition, orange the RC condition, yellow the CC condition, and purple the FC condition. The solid lines represent the data of IPD 0 and the dotted line the data of IPD  $\pi$ . Foreach condition, the goodness of fit ( $R^2$ ) with IPD of 0 was: RR( $R^2=0.2776$ ), RC( $R^2=0.1657$ ), CC( $R^2=0.2179$ ), FC( $R^2=0.2893$ ). The goodness of fit with IPD of  $\pi$  was: RR( $R^2=0.2075$ ), RC( $R^2=0.1390$ ), CC( $R^2=0.0469$ ), FC( $R^2=0.0288$ ).**

386 increment was required for the discrimination.

387 It is often assumed that the neural encoding of sound intensity is implemented by spike rate (Cai et al., 2009;  
 388 Michey et al., 2013b). However, auditory nerve fibers (ANFs) usually saturate above certain sound levels  
 389 (Bruce et al., 2018). Therefore, if the intensity JND measures are the result of rate-based encoding, an  
 390 additional mechanism must exist to combine information across ANFs (Viemeister, 1988). Several studies  
 391 have suggested that the auditory cortex plays such a role in intensity discrimination (Dykstra et al., 2012;  
 392 Michey et al., 2013a). We propose that such a mechanism could also be located at the level of the CN.  
 393 Physiological studies found neural correlates of CMR where neural activity was affected by comodulation (e.g.  
 394 Nelken et al., 1999; Pressnitzer et al., 2001; Neuert et al., 2004). One might think that at a given stimulus  
 395 level, the neural activity is higher in conditions with a masking release compared to a condition without a  
 396 masking release. In this case, it seems plausible that the internal representation of the tone rather than the  
 397 physical target tone level is relevant for sound perception. However, as the intensity JND is the same for the  
 398 same target tone level regardless of the amount of masking release, our results indicate that the physical  
 399 target tone level is encoded and preserved, in addition to the enhanced neural representation at thresholds as  
 400 an internal signal-to-noise ratio (iSNR). For the intensity encoding at the level of CN, small cells showed  
 401 preserved intensity encoding of the target tone in the presence of the noise (Hockley et al., 2022). These cells  
 402 displayed a unique rate-level function where the spike rate increases without saturation with increasing levels  
 403 up to 90 dB SPL (Hockley et al., 2022). This could be a possible mechanism of the intensity coding in  
 404 masking release conditions.

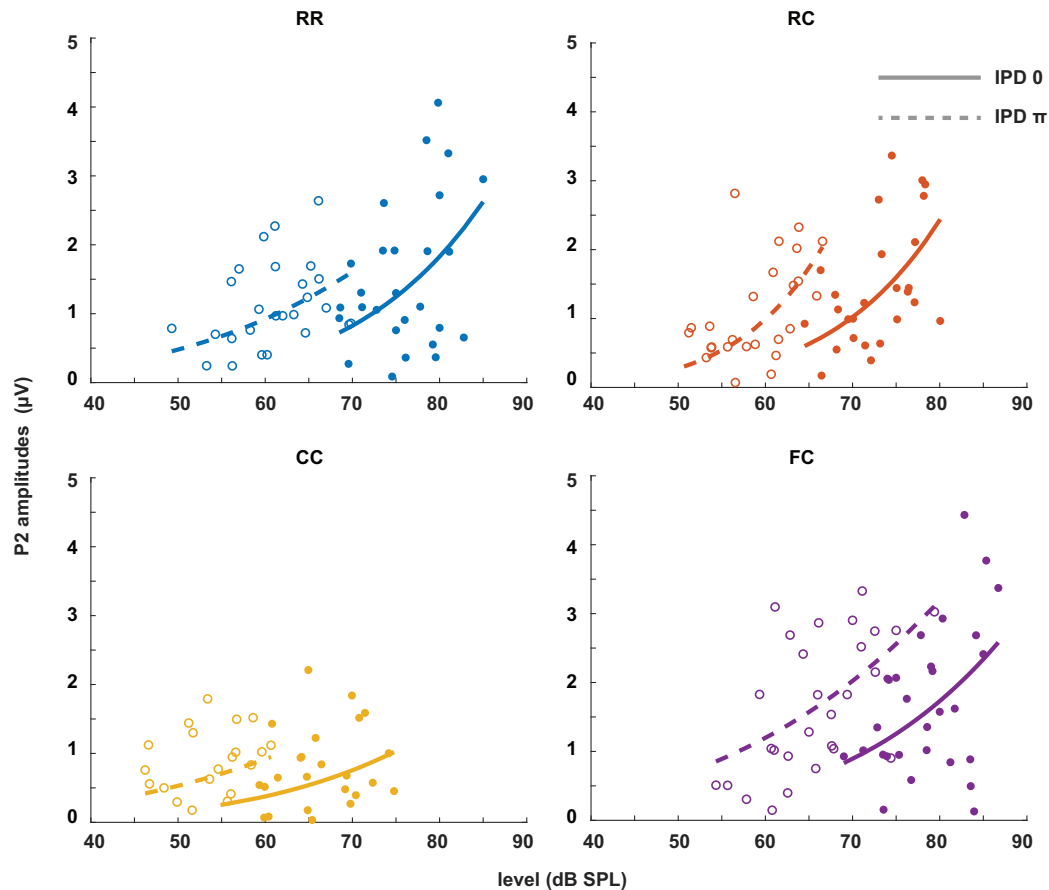


**Fig 9: P2 amplitudes as a function of target tone level at supra-threshold levels: + 15 dB, + 20 dB and + 25 dB. Individual data are plotted as single points. The data for each condition are fitted with a power function (line). Blue represents the RR condition, orange the RC condition, yellow the CC condition, and purple the FC condition. The solid lines represent the data of IPD 0 and the dotted line the data of IPD  $\pi$ . For each condition, the goodness of fit with IPD of 0 was: RR( $R^2=0.1820$ ), RC( $R^2=0.3253$ ), CC( $R^2=0.0970$ ), FC( $R^2=0.1646$ ). The goodness of fit with IPD of  $\pi$  was: RR( $R^2=0.1847$ ), RC( $R^2=0.3224$ ), CC( $R^2=0.0601$ ), FC( $R^2=0.3161$ ).**

#### 405 4.3. Estimation of salience with the intensity JND

406 We estimated salience rating based on the intensity JND measurements. The salience rating at the threshold  
 407 was set to on arbitrarily. This was based on the idea that the detection of a signal by the auditory system is  
 408 possible once the internal representation of that signal exceeds a critical iSNR. Based on linear signal theory  
 409 approach, any addition of signal energy above the detection threshold should increase the iSNR proportionally  
 410 with the increase of the signal intensity, resulting in enhanced salience (e.g., Epp and Verhey, 2009; Egger  
 411 et al., 2019). The data from the present study, however, is not in line with this hypothesis. As shown in Fig 6,  
 412 the salience increases as a function of the target tone level, but each condition shows different slopes rather  
 413 than constant slopes. This means that the change in salience is dependent on the physical target tone level  
 414 rather than the iSNR. At higher intensities, the estimated salience measures converge, indicating the vanishing  
 415 effect of the beneficial cues leading to CMR and BMLD. This suggests that beneficial cues for target detection  
 416 might not be used by the auditory system at natural conversational levels.

417 From a physiological point of view, this interpretation would imply that the physical target tone level needs to  
 418 be encoded, affecting the neural representation of the signal enhanced by the processing of comodulation and  
 419 IPD. This also clearly outlines a shortcoming of the simplified model by Epp and Verhey (2009), which does not  
 420 reflect any nonlinearity that would explain this behavioral outcome. Thus, further studies are needed to enable  
 421 us to extend this argument towards more complex signals like speech. Furthermore, it should be highlighted  
 422 that the estimated salience in the present study and in the study by Egger et al. (2019) likely reflect different

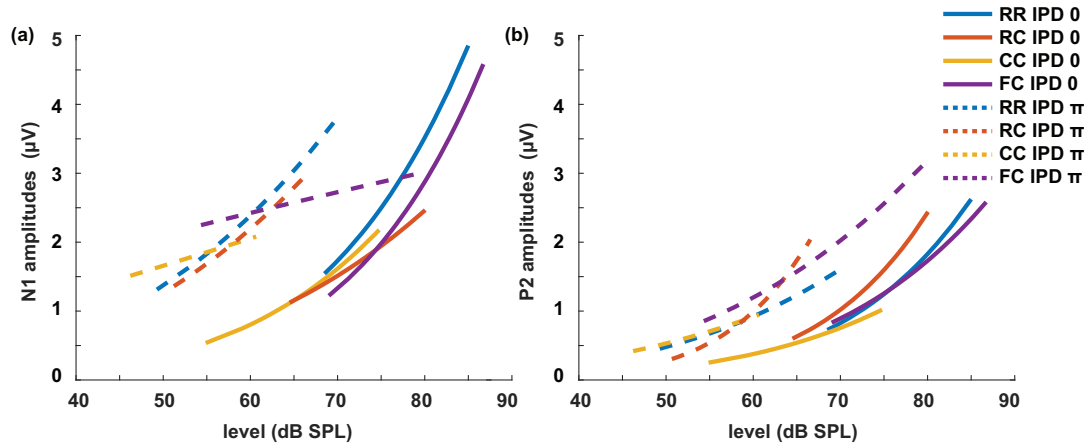


**Fig 10: The plots of the LAEPs with a function of target tone level. The data of N1 (left) and P2 (right) is fitted with the power function and plotted with the line. Blue corresponds to RR condition, orange to RC, yellow to CC, and purple to FC condition. Solid lines represent the data of IPD 0, and dotted lines represent the data of IPD  $\pi$ .**

423 aspects of perception. Egger et al. (2019) suggested that some listeners might have used a partial loudness  
 424 cue to assess the salience of the presented target tone. This is consistent with the present study in terms of  
 425 the dependence on the physical target tone level rather than the level above the masked threshold. However,  
 426 with existing loudness model, the relation between the salience and loudness growth as a function of the target  
 427 tone level in masking release conditions is unclear.

#### 428 4.4. LAEPs and intensity JNDs

429 In previous studies, the P2 component of the LAEP was suggested to be correlated with the supra-threshold  
 430 levels of the masked tone (Epp et al., 2013). They showed that P2 amplitudes were proportional to the amount  
 431 of masking release, CMR, and BMLD. Their results were based on measurement of the LAEP at fixed target  
 432 tone levels in the absence and presence of comodulation and IPD. In a follow-up study by Egger et al. (2019),  
 433 they measured P2 amplitudes at the same supra-threshold levels that were adjusted individually for all listeners.  
 434 They found that the P2 amplitudes were similar at the same level above threshold across conditions. They  
 435 noted that N1 amplitudes were correlated with the amount of BMLD. They also measured the salience of the  
 436 target tone with the continuous scaling method. However, they could not find the correlation between the P2  
 437 amplitudes and the salience ratings. In the present study, we estimated how P2 amplitudes grow as a function  
 438 of the target tone level. As shown in Fig 10, N1 amplitudes showed more prominent difference between diotic  
 439 and dichotic conditions than P2 amplitudes. However, the  $FC_{\pi}$  showed a little correlation with target tone  
 440 levels than other conditions. If N1 amplitudes reflect BMLD processing at the IC level, this might suggest an  
 441 additional higher-level BMLD processing. On the contrary, P2 amplitudes were proportional to the target tone  
 442 level in all conditions, and showed higher goodness of fit than N1 amplitudes. P2 amplitudes were larger in  
 443 dichotic conditions than diotic conditions, reflecting enhanced salience. Between conditions with the same  
 444 IPD, difference was marginal compared to estimated salience behaviorally. In addition, with a hypothesis that  
 445 the intensity JND is encoded with spike rate, we estimated LAEPs and the intensity JND measures (Fig 11).  
 446 We estimated both LAEPs and the intensity JND from the fitted function of LAEPs and intensity JNDs. We  
 447 used individual supra-threshold levels of all conditions from fifteen listeners as an input to the fitted functions.  
 448 The amplitudes of LAEPs were inversely correlated with the intensity JND measures and re-scaled JND. P2  
 449 amplitudes showed a steeper increase as the intensity JND decreases. With re-scaled JND, which showed  
 450 better correlation with the target the level (Fig 5), P2 amplitudes across conditions with same IPD were less  
 451 diverted from each other compared to the intensity JND measures. P2 amplitudes had a linear relationship to  
 452 re-scaled JND measures.

#### 453 4.5. LAEPs and salience

454 To investigate if P2 amplitudes could be a neural measure for salience, we estimated the salience at the  
 455 supra-threshold levels individually (+15 dB, + 20 dB, + 25 dB). Fig 12 shows the relation between the  
 456 estimated salience and the amplitudes of N1 and P2. Although P2 amplitudes were more correlated with

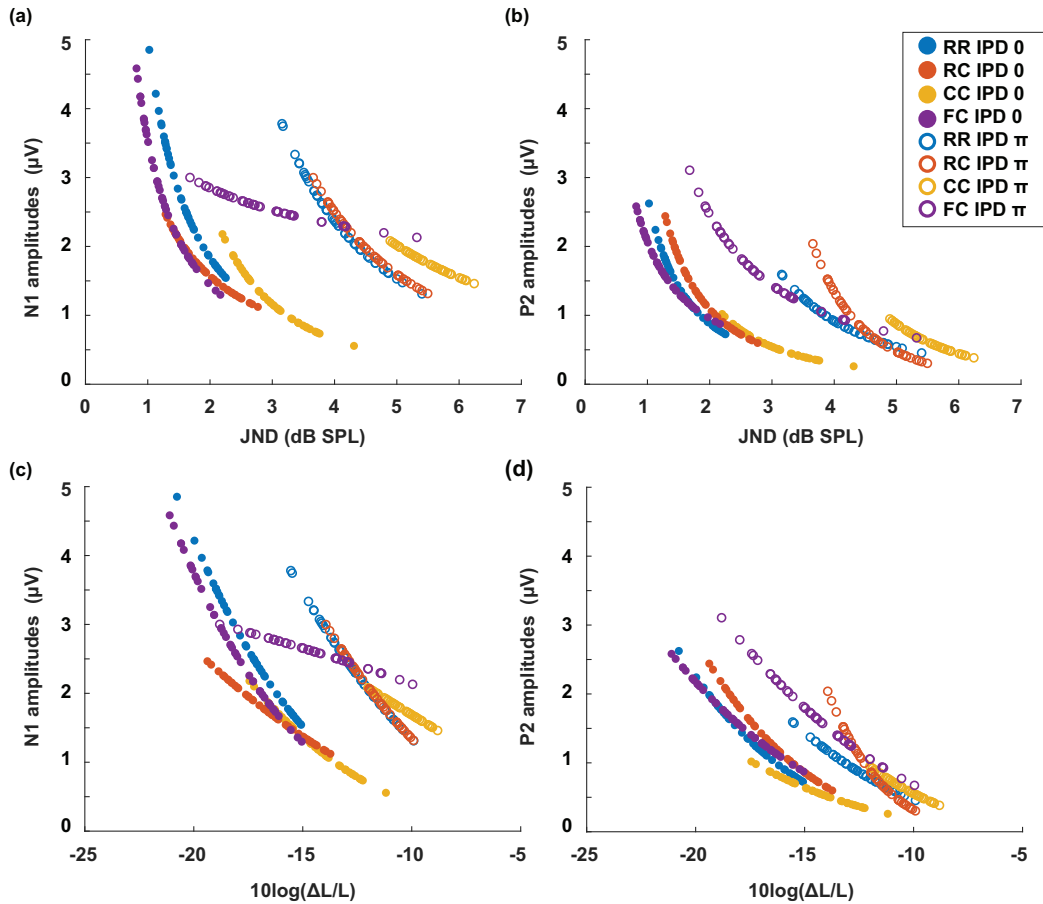


**Fig 11: LAEPs as a function of re-scaled intensity JNDs ( $\Delta L/L$ ). The data of N1 (left) and P2 (right) are fitted with a power function. The blue line represents the *RR* condition, the orange line the *RC* condition, the yellow line the *CC* condition, and the purple line the *FC* condition. The solid line represents the data for IPD of 0 and dotted lines the data for IPD of  $\pi$ .**

457 estimated salience than N1 amplitudes, two conditions showed deviating patterns in dichotic conditions (e.g.,  
 458 *RC $_{\pi}$* , *FC $_{\pi}$* ). Here, we assumed that the internal representation of the target tone in noise arises from serial  
 459 auditory processing, and the resulting iSNR is reflected in P2 amplitudes. In the first experiment, CMR and  
 460 BMLD showed non-linearity, such as reduced CMR in dichotic conditions and a strong correlation between  
 461 CMR and BMLD in the *FC* dichotic conditions. In the second experiment, the intensity JND showed high  
 462 variance in low target level compared to the re-scaled JND measures. As estimated salience was based on  
 463 the intensity JND measures, this might have affected the accuracy of the salience rating. Therefore, salience  
 464 estimation based on re-scaled JND measures may produce a better prediction. However, the method for  
 465 translating re-scaled JND measures to salience measures needs to be further investigated. In the third  
 466 experiment, N1 amplitudes were not correlated with the audibility, or BMLD processing, in the *FC $_{\pi}$*   
 467 condition. This also suggests a possible higher-order auditory processing that may play a role in shaping neural  
 468 responses. As the neural mechanisms underlying such non-linearity is unclear, further physiological evidence  
 469 is needed to make a clear conclusion on how much extent P2 amplitudes can reflect the auditory processing  
 470 stages and predict the salience. If additional high-level auditory processing is involved in combining CMR and  
 471 BMLD together with temporal integration, AEPs that elicited later than P2 (e.g., P300) might provide more  
 472 insights on the feasibility of electrophysiological measures for the salience.



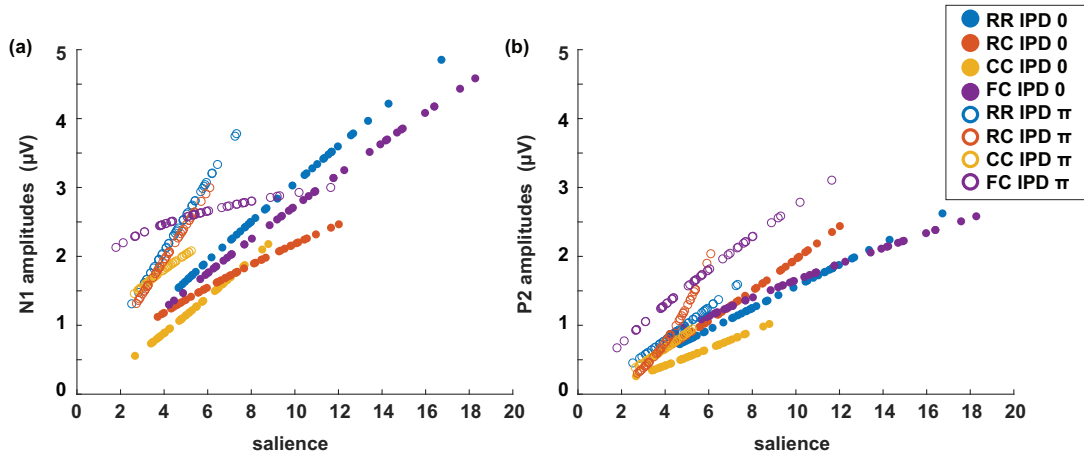


**Fig 12: Estimated salience correlated with a) the N1 amplitude of the LAEP, and b) the P2 amplitude of the LAEP.**

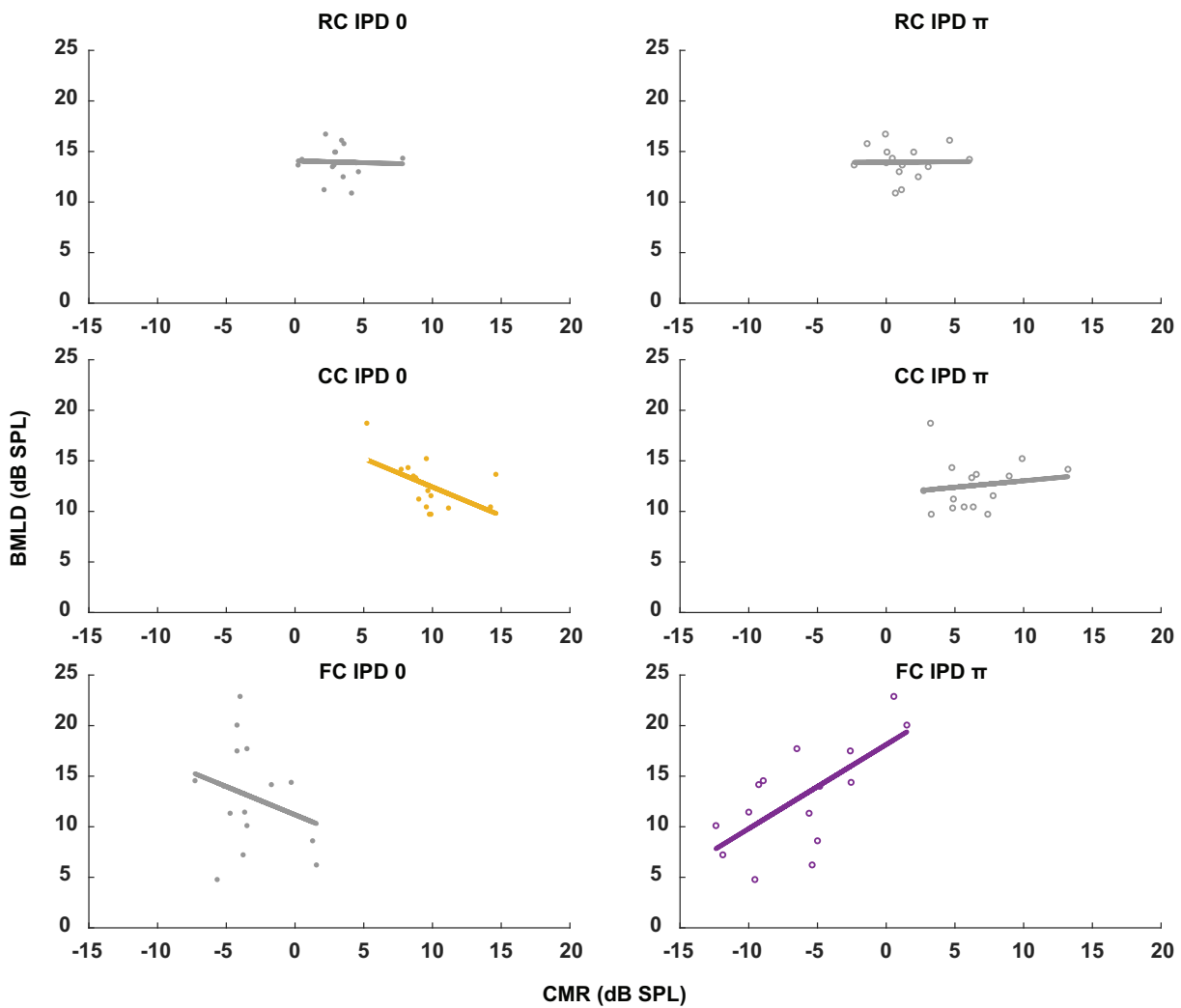


**Fig 13: Linear regression analysis between CMR and BMLD for all stimulus conditions. Only the conditions with significant p-values were plotted with color (see Table 1).**

## 473 5. Conclusion

474 In this study, we investigated the detection and discrimination of masked tones in masking release conditions.  
475 Auditory cues such as comodulation and IPD, and the preceding masker, could enhance the detection  
476 performance. On the other hand, at supra-threshold levels, the discrimination performance was highly  
477 dependent on the physical target tone level. Regardless of the masking release conditions, the intensity JND  
478 measures were correlated with the target tone level. Furthermore, the estimated salience was higher in  
479 conditions with lower detection thresholds. At the high level, however, estimated salience converged to the  
480 same value across conditions. Lastly, the P2 amplitudes were more correlated with the behavioral measure of  
481 the salience than the L1 amplitudes.

$$y = a * x + b$$

		<i>a</i>	<i>b</i>	<i>p-values</i>
<b>diotic</b>	<b>RC</b>	-0.04	14.08	0.886
	<b>CC</b>	-0.56	18.05	0.044*
	<b>FC</b>	-0.56	11.18	0.338
<b>dichotic</b>	<b>RC</b>	0.01	13.95	0.968
	<b>CC</b>	0.13	11.75	0.610
	<b>FC</b>	0.83	18.13	0.006*

**Table 1: Linear regression summary for all conditions. *a* is CMR *b* is BMLD.**

## 482 Acknowledgments

483 We would like to thank Viktorija Ratkute for support with the data collection.

## 484 References

- 485 Asilador, A. and Llano, D. A. (2021). Top-down inference in the auditory system: Potential roles for  
486 corticofugal projections. *Frontiers in Neural Circuits*, page 89.
- 487 Bruce, I. C., Erfani, Y., and Zilany, M. S. (2018). A phenomenological model of the synapse between the inner  
488 hair cell and auditory nerve: Implications of limited neurotransmitter release sites. *Hearing research*,  
489 360:40–54.
- 490 Cai, S., Ma, W.-L. D., and Young, E. D. (2009). Encoding intensity in ventral cochlear nucleus following  
491 acoustic trauma: implications for loudness recruitment. *Journal of the Association for Research in*  
492 *Otolaryngology*, 10(1):5–22.
- 493 Cohen, M. F. and Schubert, E. D. (1991). Comodulation masking release and the masking-level difference.  
494 *The Journal of the Acoustical Society of America*, 89(6):3007–3008.
- 495 Dau, T., Ewert, S., and Oxenham, A. J. (2009). Auditory stream formation affects comodulation masking  
496 release retroactively. *The Journal of the Acoustical Society of America*, 125(4):2182–2188.
- 497 Dau, T., Ewert, S. D., and Oxenham, A. J. (2005). Effects of concurrent and sequential streaming in  
498 comodulation masking release. In *Auditory signal processing*, pages 334–342. Springer.
- 499 Dykstra, A. R., Koh, C. K., Braida, L. D., and Tramo, M. J. (2012). Dissociation of detection and discrimination  
500 of pure tones following bilateral lesions of auditory cortex.
- 501 Egger, K., Dau, T., and Epp, B. (2019). Supra-threshold perception and neural representation of tones  
502 presented in noise in conditions of masking release. *Plos one*, 14(10):e0222804.
- 503 Epp, B. and Verhey, J. L. (2009). Superposition of masking releases. *Journal of computational neuroscience*,  
504 26(3):393–407.
- 505 Epp, B., Yasin, I., and Verhey, J. L. (2013). Objective measures of binaural masking level differences and  
506 comodulation masking release based on late auditory evoked potentials. *Hearing research*, 306:21–28.

- 507 Ernst, S. M. and Verhey, J. L. (2006). Role of suppression and retro-cochlear processes in comodulation  
508 masking release. *The Journal of the Acoustical Society of America*, 120(6):3843–3852.
- 509 Ewert, S. D. (2013). Afc—a modular framework for running psychoacoustic experiments and computational  
510 perception models. In *Proceedings of the international conference on acoustics AIA-DAGA*, pages  
511 1326–1329.
- 512 Grose, J. H., Buss, E., and Hall III, J. W. (2009). Within-and across-channel factors in the multiband  
513 comodulation masking release paradigm. *The Journal of the Acoustical Society of America*,  
514 125(1):282–293.
- 515 Guinan Jr, J. J. (2006). Olivocochlear efferents: anatomy, physiology, function, and the measurement of  
516 efferent effects in humans. *Ear and hearing*, 27(6):589–607.
- 517 Hall, J. W., Haggard, M. P., and Fernandes, M. A. (1984). Detection in noise by spectro-temporal pattern  
518 analysis. *The Journal of the Acoustical Society of America*, 76(1):50–56.
- 519 Hall III, J. W., Buss, E., and Grose, J. H. (2011). Exploring the additivity of binaural and monaural masking  
520 release. *The Journal of the Acoustical Society of America*, 129(4):2080–2087.
- 521 Hockley, A., Wu, C., and Shore, S. E. (2022). Olivocochlear projections contribute to superior intensity coding  
522 in cochlear nucleus small cells. *The Journal of physiology*.
- 523 Kreft, H. A., Wojtczak, M., and Oxenham, A. J. (2018). Auditory enhancement under simultaneous masking in  
524 normal-hearing and hearing-impaired listeners. *The Journal of the Acoustical Society of America*,  
525 143(2):901–910.
- 526 Levitt, H. (1971). Transformed up-down methods in psychoacoustics. *The Journal of the Acoustical society of*  
527 *America*, 49(2B):467–477.
- 528 Micheyl, C., Kreft, H., Shamma, S., and Oxenham, A. J. (2013a). Temporal coherence versus harmonicity in  
529 auditory stream formation. *The Journal of the Acoustical Society of America*, 133(3):EL188–EL194.
- 530 Micheyl, C., Schrater, P. R., and Oxenham, A. J. (2013b). Auditory frequency and intensity discrimination  
531 explained using a cortical population rate code. *PLoS computational biology*, 9(11):e1003336.
- 532 Nelken, I., Rotman, Y., and Yosef, O. B. (1999). Responses of auditory-cortex neurons to structural features of  
533 natural sounds. *Nature*, 397(6715):154–157.
- 534 Nelson, P. C. and Young, E. D. (2010). Neural correlates of context-dependent perceptual enhancement in the  
535 inferior colliculus. *Journal of Neuroscience*, 30(19):6577–6587.
- 536 Neuert, V., Verhey, J. L., and Winter, I. M. (2004). Responses of dorsal cochlear nucleus neurons to signals in  
537 the presence of modulated maskers. *Journal of Neuroscience*, 24(25):5789–5797.
- 538 Oertel, D., Wright, S., Cao, X.-J., Ferragamo, M., and Bal, R. (2011). The multiple functions of t  
539 stellate/multipolar/chopper cells in the ventral cochlear nucleus. *Hearing research*, 276(1-2):61–69.
- 540 Oostenveld, R., Fries, P., Maris, E., and Schoffelen, J.-M. (2011). Fieldtrip: open source software for  
541 advanced analysis of meg, eeg, and invasive electrophysiological data. *Computational intelligence and*  
542 *neuroscience*, 2011.
- 543 Ozimek, E. and Zwislocki, J. J. (1996). Relationships of intensity discrimination to sensation and loudness  
544 levels: Dependence on sound frequency. *The Journal of the Acoustical Society of America*,  
545 100(5):3304–3320.
- 546 Pressnitzer, D., Meddis, R., Delahaye, R., and Winter, I. M. (2001). Physiological correlates of comodulation  
547 masking release in the mammalian ventral cochlear nucleus. *Journal of Neuroscience*, 21(16):6377–6386.
- 548 Raphael, L. J., Borden, G. J., and Harris, K. S. (2007). *Speech science primer: Physiology, acoustics, and*  
549 *perception of speech*. Lippincott Williams & Wilkins.

- 550 Riedel, H., Granzow, M., and Kollmeier, B. (2001). Single-sweep-based methods to improve the quality of  
551 auditory brain stem responses part ii: Averaging methods. *Zeitschrift fur Audiologie*, 40(2):62–85.
- 552 Schooneveldt, G. P. and Moore, B. C. (1989). Comodulation masking release for various monaural and  
553 binaural combinations of the signal, on-frequency, and flanking bands. *The Journal of the Acoustical  
554 Society of America*, 85(1):262–272.
- 555 Shackleton, T. M., Arnott, R. H., and Palmer, A. R. (2005). Sensitivity to interaural correlation of single  
556 neurons in the inferior colliculus of guinea pigs. *Journal of the Association for Research in Otolaryngology*,  
557 6(3):244–259.
- 558 Shackleton, T. M., Skottun, B. C., Arnott, R. H., and Palmer, A. R. (2003). Interaural time difference  
559 discrimination thresholds for single neurons in the inferior colliculus of guinea pigs. *Journal of  
560 Neuroscience*, 23(2):716–724.
- 561 Sollini, J. and Chadderton, P. (2016). Comodulation enhances signal detection via priming of auditory cortical  
562 circuits. *Journal of Neuroscience*, 36(49):12299–12311.
- 563 Terreros, G. and Delano, P. H. (2015). Corticofugal modulation of peripheral auditory responses. *Frontiers in  
564 systems neuroscience*, 9:134.
- 565 van de Par, S. and Kohlrausch, A. (1999). Dependence of binaural masking level differences on center  
566 frequency, masker bandwidth, and interaural parameters. *The Journal of the Acoustical Society of  
567 America*, 106(4):1940–1947.
- 568 Verhey, J. L. and Heeren, W. (2015). Categorical scaling of partial loudness in a condition of masking release.  
569 *The Journal of the Acoustical Society of America*, 138(2):904–915.
- 570 Viemeister, N. F. (1988). Intensity coding and the dynamic range problem. *Hearing research*, 34(3):267–274.
- 571 Zohar, O., Shackleton, T. M., Nelken, I., Palmer, A. R., and Shamir, M. (2011). First spike latency code for  
572 interaural phase difference discrimination in the guinea pig inferior colliculus. *Journal of Neuroscience*,  
573 31(25):9192–9204.